OPEN

PRS GLOBAL OPEN

EXPERIMENTAL

Functional Validation of a New Alginate-based Hydrogel Scaffold Combined with Mesenchymal Stem Cells in a Rat Hard Palate Cleft Model

Marie Naudot, PhD*
Julien Davrou, MD*†‡
Az-Eddine Djebara, MD§
Anaïs Barre, MS*
Nolwenn Lavagen, MD*‡¶
Sandrine Lardière, PhD‖
Soufiane Zakaria Azdad, MD**
Luciane Zabijak, BS††
Stéphane Lack, PhD‖
Bernard Devauchelle, MD*‡¶
Jean-Pierre Marolleau, MD‡‡‡§§
Sophie Le Ricousse, PhD*‡

Background: One of the major difficulties in cleft palate repair is the requirement for several surgical procedures and autologous bone grafting to form a bony bridge across the cleft defect. Engineered tissue, composed of a biomaterial scaffold and multipotent stem cells, may be a useful alternative for minimizing the non-negligible risk of donor site morbidity. The present study was designed to confirm the healing and osteogenic properties of a novel alginate-based hydrogel in palate repair.

Methods: Matrix constructs, seeded with allogeneic bone marrow–derived mesenchymal stem cells (BM-MSCs) or not, were incorporated into a surgically created, critical-sized cleft palate defect in the rat. Control with no scaffold was also tested. Bone formation was assessed using microcomputed tomography at weeks 2, 4, 8, and 12 and a histologic analysis at week 12.

Results: At 12 weeks, the proportion of bone filling associated with the use of hydrogel scaffold alone did not differ significantly from the values observed in the scaffold-free experiment (61.01% ± 5.288% versus 36.91% ± 5.132%; $p = 0.1620$). The addition of BM-MSCs stimulated bone formation not only at the margin of the defect but also in the center of the implant.

Conclusions: In a relevant in vivo model of cleft palate in the rat, we confirmed the alginate-based hydrogel's biocompatibility and real advantages for tissue healing. Addition of BM-MSCs stimulated bone formation in the center of the implant, demonstrating the new biomaterial's potential for use as a bone substitute grafting material for cleft palate repair. *(Plast Reconstr Surg Glob Open 2020;8:e2743; doi: 10.1097/GOX.0000000000002743; Published online 29 April 2020.)*

INTRODUCTION

Cleft lip and alveolar cleft with or without cleft palate are the most common human craniofacial malformations at birth. The prevalence of these defects is around 1 in 500–700 live births but varies as a function of geographic origin, ethnic group, environmental factors, and socioeconomic factors.[1] A wide range of surgical techniques has been described for the treatment of clefts and other palate defects.[2,3] Patients will typically need several surgical procedures to obtain complete closure of the cleft. A bone graft harvested from hip bone is frequently required. Hence, there is a need for alternative approaches that can replace bone grafts and avoid or overcome the disadvantages associated with bone harvesting from an additional donor site (eg, a longer operating time, prolonged recovery, and greater donor site morbidity, including pain and neurosensory impairments). Engineered tissue, composed of a biomaterial scaffold and multipotent stem cells, is a novel treatment option.[4] A few preclinical studies have evaluated the potential value of novel bone-substitute materials for bone regeneration in the oral cavity.[5,6] Some positive clinical results have already been published.[7–9] However,

*From the *Research Unit 7516, CHIMERE, Jules Verne University of Picardie, Amiens, France; †Department of Maxillofacial Surgery, Pitié Salpêtrière Hospital, AP-HP, Paris, France; ‡Facing Faces Institute, Amiens, France; §Department of Orthopaedic Surgery, Amiens University Hospital, Amiens, France; ¶Department of Maxillofacial Surgery, Amiens University Hospital, Amiens, France; ‖R&D Department, Les Laboratoires Brothier, Nanterre, France; **Department of Pathology and Cytology, Amiens University Hospital, Amiens, France; ††Platform ICAP, Jules Verne University of Picardie, Amiens, France; ‡‡‡Research Unit 4666, HEMATIM, Jules Verne University of Picardie, Amiens, France; and §§Department of Haematology, Amiens University Hospital, Amiens, France.*

Received for publication September 26, 2019; accepted February 5, 2020.

Drs. Naudot and Davrou contributed equally to this study.

DOI: 10.1097/GOX.0000000000002743

Disclosure: *M.N., J.D., Az.-E.D., N.L., S.Z.A., and L.Z. declare that they have no competing or commercial interests. A.B., B.D., J.P.M. and S.L.R. are cited as co-inventors on the corresponding patent (FR Patent 1854630 issued May 30, 2018). They declare that they have no other competing interests. S.L. and S.L. are employed by the Laboratoires Brothier.*

the novel grafting materials have sometimes failed to demonstrate any superiority compared with conventional autologous bone graft.[10–12]

At present, autologous osteoblasts[13,14] and bone marrow–derived stem cells[15,16] are the most commonly used seed cells in regenerative approaches to alveolar cleft defect repair. Because cleft malformations are often diagnosed during a prenatal ultrasound scan, mesenchymal stem cells (MSCs) from the umbilical cord could be used as a donor source with no associated morbidity or ethical concerns.

A range of biomaterials and engineered bone tissues have also been tested in animals for the treatment of cleft palate,[17,18] but the clinical results have not always been conclusive.[9] Biomaterial-based scaffold provides an architectural blueprint for cell regeneration and ideally possesses osteoconductive, osteoinductive, and/or osseointegration properties. As a natural, nonthrombogenic hydrogel with good biocompatibility and biodegradability, alginate has been used for cell delivery or as a protein carrier in bone tissue engineering applications.[19,20]

In previous work, we demonstrated the high in vivo angiogenic capacity and osteogenic potential of a new alginate-based hydrogel (data submitted for publication). It was able to act as a cell depot and protected transplanted cells. In the present study, we evaluated the in vivo effect of seeding the biomaterial with murine bone marrow–derived MSCs (BM-MSCs) on wound healing and osteogenesis in a dedicated rat cleft palate model. Bone formation was assessed using microcomputed tomography (μCT) at weeks 2, 4, 8, and 12 and a histologic analysis at week 12.

MATERIALS AND METHODS

Biomaterial Production

Alginate-based hydrogel scaffolds were synthesized as described in the patent.[21] The hydrogel was prepared in 2 steps, under sterile conditions. First, nonwoven calcium alginate (Les Laboratoires Brothier, Nanterre, France) was mixed with a trisodium citrate solution (10 g/L) (VWR chemicals, Fontenay-sous-Bois, France) to initiate cross-linking and gel formation. Second, sodium alginate (1.5%) (Kimica, Tokyo, Japan) was added to the gel to produce a macroporous scaffold.

Cell Isolation and Culture

Marrow cells were obtained from the bone shaft of the femurs and the tibias of 8-week-old male Sprague Dawley rats and expanded in vitro in growth medium α Modified Eagle's Medium (Sigma-Aldrich, Saint-Quentin Fallavier, France) supplemented with 10% fetal bovine serum, 2-mM L-glutamine, and 1% antibiotics (100 U/mL penicillin and 100 pg/mL streptomycin). All supplements were purchased from Eurobio (Courtaboeuf, France). The cells were cultured in a humidified 5% carbon dioxide (CO_2) atmosphere at 37°C. Nonadherent cells were removed after 2 days, and fresh medium was added.

Animals and Surgical Procedures

All animal experiments were approved by the local Animal Care and Use Committee and the French Ministry of Research (registration number: APAFIS#10364-2017062609484123 v3).

Twenty-seven 8-week-old Sprague Dawley rats (Janvier Labs, Le Genest-Saint-Isle, France) were housed in ventilated cabinets under controlled conditions, with ad libitum access to chow and water. For cell culture, scaffolds (0.25 cm^2) were washed twice with growth medium at 37°C (once for 1.5 hours, and then overnight) to neutralize the pH. BM-MSCs (5×10^5) were seeded into the scaffold and allowed to adhere for 2 hours. Fresh medium was added to wells containing scaffolds, and the cells were cultured for 24 hours at 37°C in a 5% CO_2 atmosphere. Matrix constructs were then engrafted into the palate lesion. Animals were anesthetized by intraperitoneal injection of a mixture of ketamine (100 mg/kg) and xylazine (10 mg/kg) and placed in dorsal decubitus. Incisions were performed transversally through the mucosa and periosteum layers 1 mm on the mesial side of the first molars. A mucoperiosteal flap was raised by following the palatal sulcus bilaterally up to the distal part of the hard palate and by preserving the palatal branches of the maxilla artery. A bone defect in the hard palate was created between the molars using a trephine. The alveolar processes were preserved on both sides, and the full-thickness bone fragment was removed to expose the mucous membranes of the nasal fossae. The bone defect was left uncovered (controls with no hydrogel; n = 11) or covered with the scaffold alone (n = 8) or the scaffold seeded with MSCs (n = 8). The palatal mucoperiosteal flap was then replaced in situ and fixed with 3 stitches of absorbable suture (Vicryl 5/0; Ethicon, Issy-les-Moulineaux, France). Analgesia was achieved through subcutaneous injections of buprenorphine (0.2 mg/kg, Buprecare®; Centravet, Nancy, France) twice a day for 2 days. At the end point (12 weeks), all rats were euthanized using CO_2. The maxillae were dissected and fixed in 4% neutral buffered formalin.

In Vivo μCT Assessment and Radiomorphometric Analysis

Rats were anesthetized (induction with 5% isoflurane at an airflow of 1 L/min, and maintenance with 3% isoflurane at 0.5 L/min). The animals were imaged using an x-ray μCT device (SKYSCAN 1176; Bruker, Kontich, Belgium; x-ray source: 65 kV, 380 μA, 1-mm Alu filter, and a 0.6° rotation step). Three-dimensional images were acquired with a maximum voxel size of 18 μm. The full 3D high-resolution raw dataset was obtained by rotating the flat panel detector 180° around the sample (scanning time: 5 minutes). An internal density phantom (calibrated in grams per cubic centimeter of hydroxyapatite) was used to scale the bone density. Three-dimensional renderings were extracted from the data frames using Dataviewer software (Bruker). A global thresholding of gray value (68–255) was performed to separate mineralized elements from background noise. Defects and regenerated bone were measured using CT scan Analyzer software (Bruker). An overall volume of interest (VOI) in the defect area was drawn by interpolating 2D regions of interest on consecutive sections. This VOI comprised the remodeled bone

defect area and was specific for the shape of the lesion in each rat. The following parameters were analyzed: bone volume (cubic millimeter), bone volume fraction (as a percentage of the total volume), and the bone mineral density (grams per square centimeter). The parameters were standardized against the volume of bone in the VOI before surgery. Parameters in the figures are quoted as the percentage of new bone and the percentage of bone mineralization. Three-dimensional images of the brain cavity were reconstructed with CTvox (Bruker microCT).

Statistical Analysis

The results in each group were quoted as the mean ± standard error of the mean. The statistical significance of intergroup differences was probed in a Kruskal–Wallis test after Dunn's correction for multiple comparisons. The following thresholds for statistical significance were considered: $*P < 0.05$, $**P < 0.01$, and $***P < 0.001$. All statistical analyses were performed using GraphPad Prism software (version 6; GraphPad Software, San Diego, Calif., USA).

Histologic Analyses

Fixed samples were immersed in Microdec EDTA A1 decalcification solution (Microm Microtech, Brignais, France) for 7 days and were then dehydrated in graded ethanol solutions. Samples were then embedded in paraffin, prepared as 3-µm sections, and stained with hematoxylin and eosin (H&E) reagent. The images were acquired using a Leica SCN 400 Slide Scanner (Leica Microsystems, Nanterre, France).

RESULTS

Animal Model: Postoperative Recovery

Although operated rats tolerated the surgery well, 3 animals died as a result of anesthetic shock. During the recovery period, 3 other animals lost a substantial amount of weight and had to be euthanized for ethical reasons: one animal in the scaffold + MSCs group died at week 4 and 2 control animals (no grafts) died at week 5. In all 3 cases, the palates were found to be perforated—probably in relation to food intake. None of the other animals

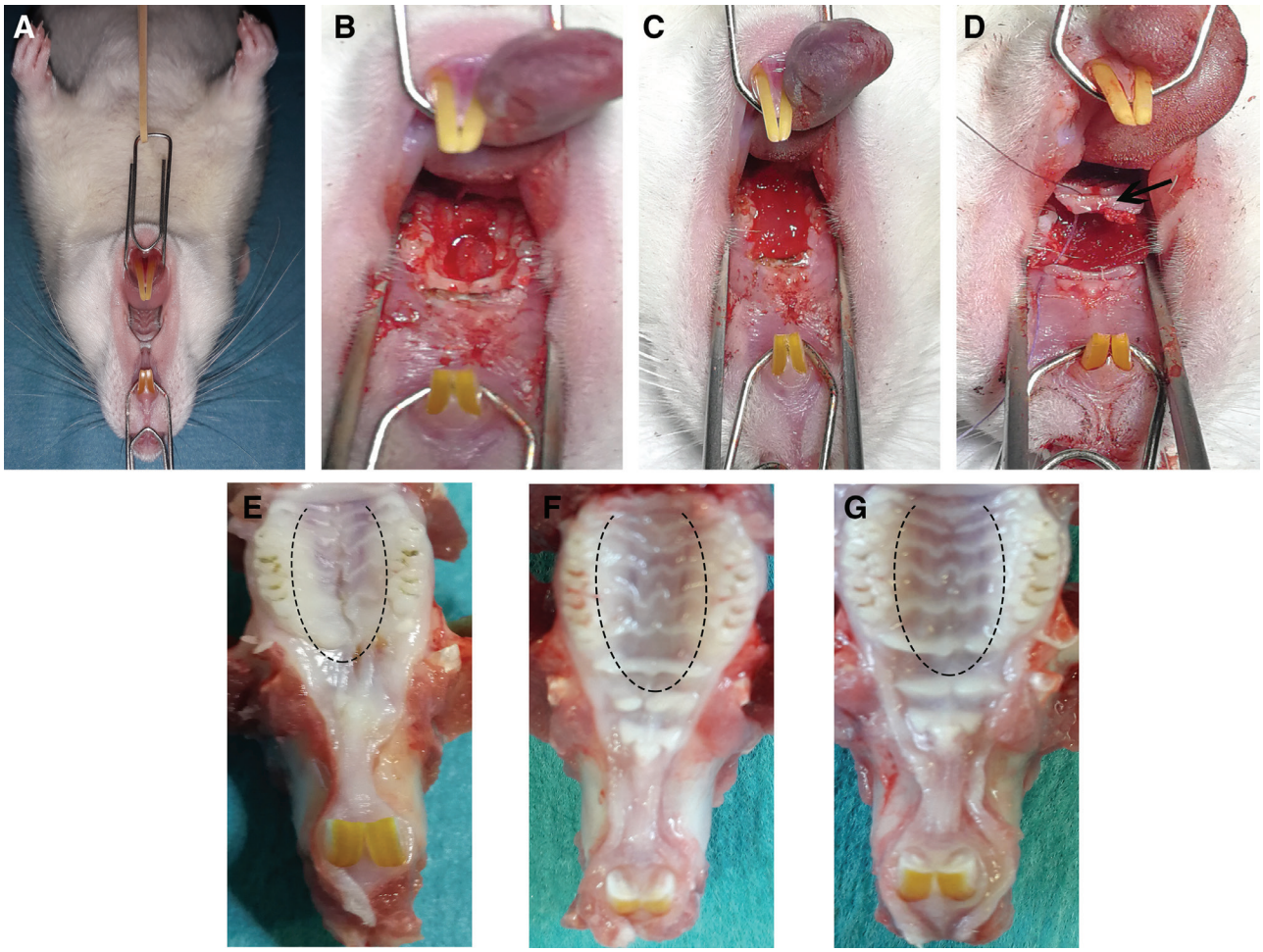

Fig. 1. Surgical creation of a cleft defect and implantation technique. A, The rat was placed in the supine position, with the tongue and cheek retracted to expose the gingival mucosa. B, A hard palate bone defect was created between the molars. C, Implantation of the scaffold into the defect. D, Repositioning of the mucoperiosteal palatal flap (black arrow) and suturing. E–G, The macroscopic appearance of the palate soft tissues in each study group. E, Controls (no graft). F, Scaffold only. G, Scaffold + MSCs (dashed line: the position of the flap-raising incision).

showed behavioral disturbances or complications during the postsurgery recovery period. After losing weight during the first week postsurgery (50 g on average), all the remaining animals gained weight steadily. The different steps in the surgery are described in Figure 1A–D. The intergroup differences in the size of the lesion were not statistically significant (Table 1).

Table 1. Mean Lesion Dimensions Immediately after Surgery in the 3 Treatment Groups (Controls: n = 8; Scaffold Only: n = 6; Scaffold + MSCs: n = 7)

	Length (mm)	Width (mm)	Area (mm^2)
Control	7.75 ± 0.93	2.85 ± 0.25	20.61 ± 3.00
Scaffold	7.18 ± 0.90	2.70 ± 0.22	18.17 ± 2.65
Scaffold + MSCs	8.46 ± 0.61	2.83 ± 0.11	23.01 ± 2.60

Representative macroscopic images of the recovered maxillae are shown in Figure 1E–G. In comparison to the control group [in which retraction of the scar can be observed (Fig. 1E)], the lesions in the scaffold-only and scaffold + MSCs groups healed much better; the palatal mucosa had a natural aspect, with no retraction (Fig. 1F, G).

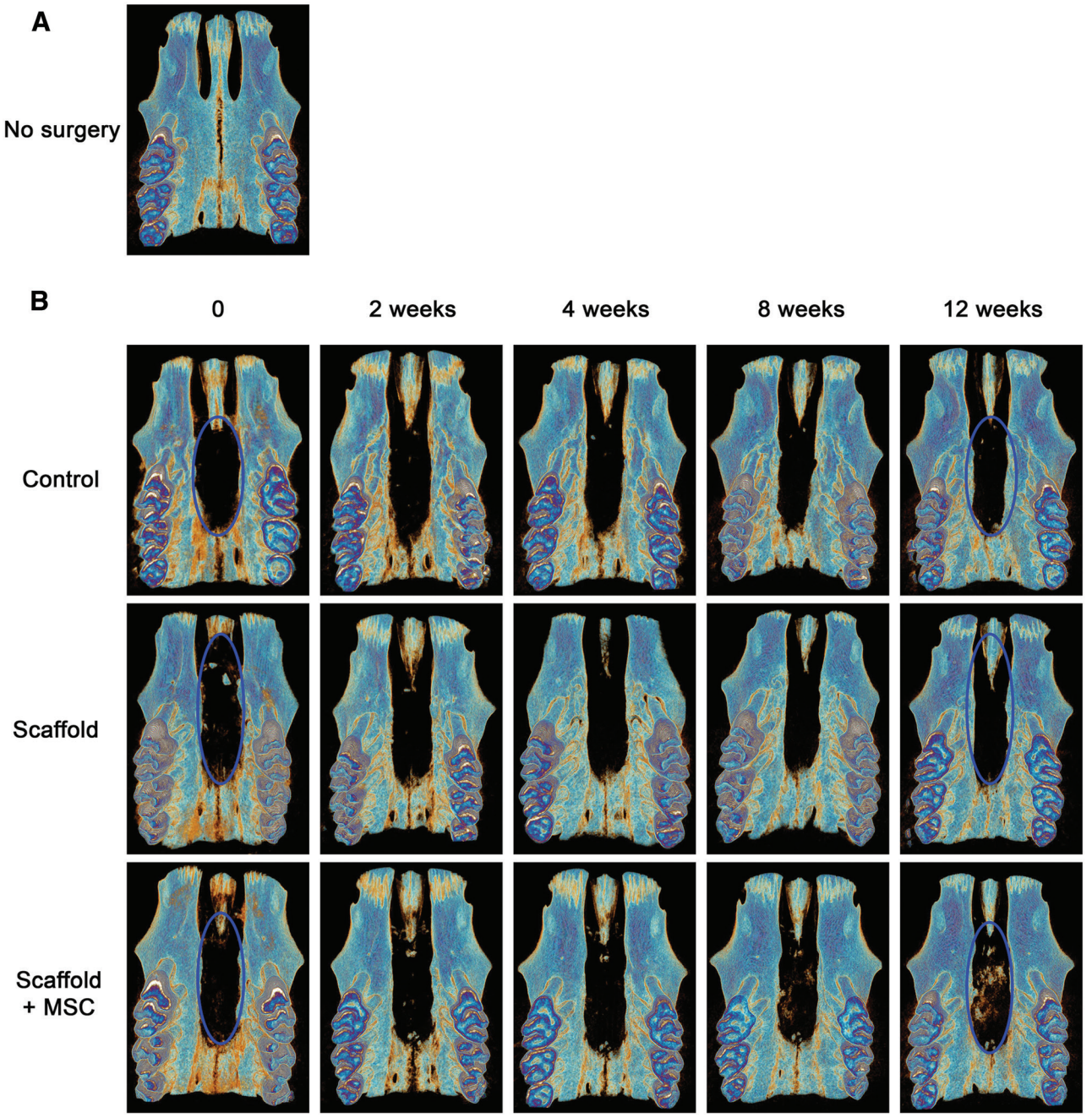

Fig. 2. Representative μCT images of bone regeneration over time (the same rat at weeks 0, 2, 4, 8, and 12) after various treatments (B). Healed cleft palates 0, 2, 4, 8, and 12 weeks after surgery in the control (no graft), scaffold-only, and scaffold + MSCs groups.

Bone Healing in the Treatment Groups

Bone regeneration in the 3 treatment groups was monitored using in vivo µCT at weeks 0, 2, 4, 8, and 12. The results showed that none of the animals in any of the groups had completely closed the defect through new bone formation, and that the control group (no graft) did not heal spontaneously over the course of the study (Fig. 2). We observed bone healing at the defect margins in all groups and toward the center of the defect (blue circle, Fig. 2B). However, bone regrowth was limited—especially in the scaffold + MSCs group. The presence of calcified material at the center of the defect was only observed in the scaffold + MSCs group as early as week 8 (Fig. 2B). The intergroup differences in bone regeneration were especially

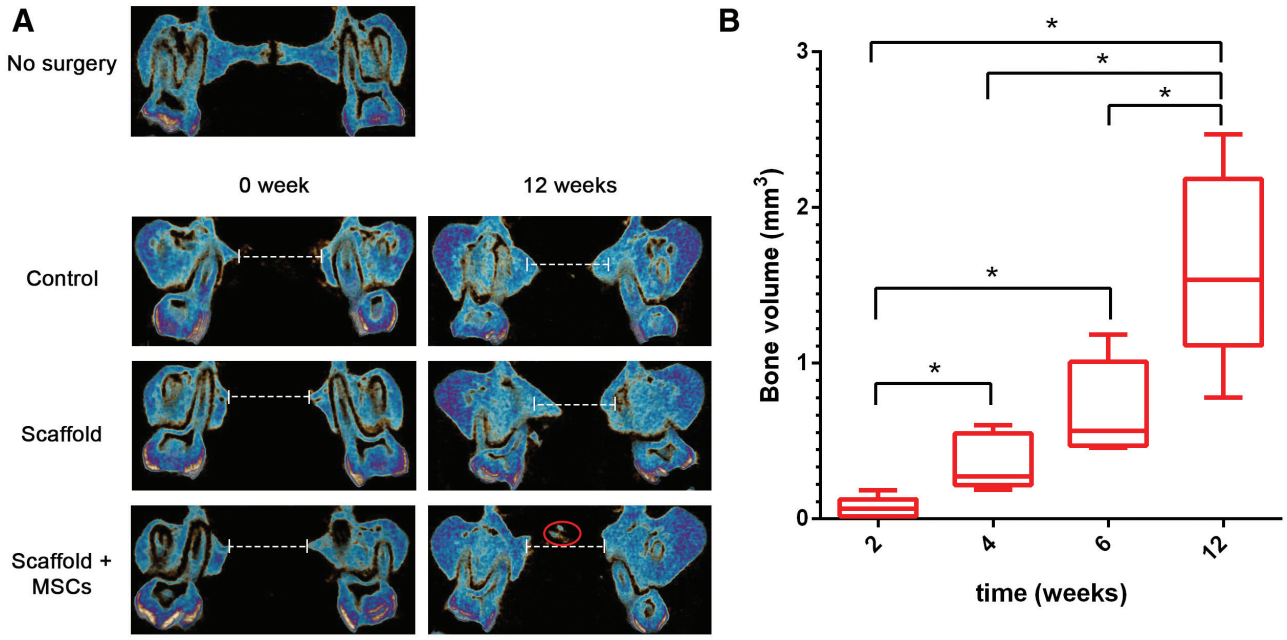

Fig. 3. A representative coronal view of the defect area (delimited by a dashed white line) in each group at the time of the surgery and at the end of the study (A). Calcium material is indicated by the red circle. A box plot of bone volume (cubic millimeter) in the area between the defect margins at weeks 2, 4, 8, and 12 in the scaffold + MSCs group (B).

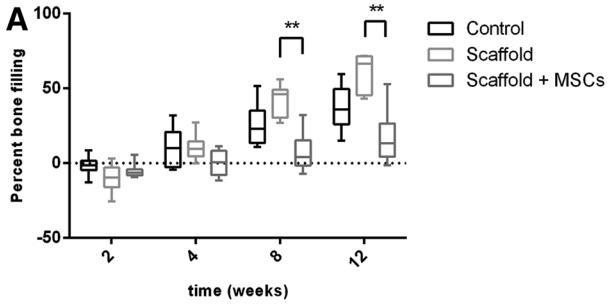

B

% bone filling					
	N	2 weeks	4 weeks	8 weeks	12 weeks
Control	8	-1.649 ± 2.189	10.43 ± 4.534	25.49 ± 4.94	36.91 ± 5.132
Scaffold	6	-9.962 ± 3.923	10.44 ± 3.717	42.3 ± 4.427	61.01 ± 5.288
Scaffold + MSCs	7	-4.52 ± 1.8	0.7085 ± 3.45	7.32 ± 4.933	17.24 ± 6.886

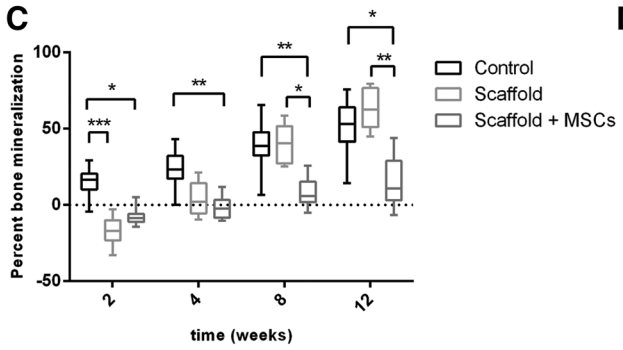

D

% bone mineralization					
	N	2 weeks	4 weeks	8 weeks	12 weeks
Control	8	15.03 ± 3.5	23.27 ± 4.473	38.92 ± 5.893	50.98 ± 6.656
Scaffold	6	-16.91 ± 4.013	3.96 ± 4.593	40.51 ± 5.363	63.14 ± 5.497
Scaffold + MSCs	7	-6.641 ± 2.132	-0.767 ± 2.925	7.711 ± 3.791	15.21 ± 6.489

Fig. 4. Percentage of bone filling (A, B) and bone mineralization (C, D) following various treatments at weeks 2, 4, 8, and 12 in the control (no graft), scaffold-only, and scaffold + MSCs groups.

clear when coronal sections were examined, with a reduction in the size of the defect (delimited by a dashed white line in Fig. 3A). In the scaffold + MSCs group, the bone volume in the area between the defect margins increased significantly over time (Fig. 3B).

A slight bone loss was observed in all groups at week 2, probably due to trauma during surgery (Fig. 4A, B). From week 8 onward, the percentage of bone filling was higher in the scaffold-only group than in the control group (week 8: 42.3% ± 4.42% versus 25.5% ± 4.94%, respectively; week 12: 61.01% ± 5.28% versus 36.91% ± 5.13%, respectively), although the differences were not statistically significant. Likewise, there were no significant differences in the percentage of bone mineralization (Fig. 4C, D) between the control group (no graft) and the scaffold-only group (week 8: 38.92% ± 5.89% versus 40.51% ± 5.36%/week 12: 50.98% ± 6.65% versus 63.14% ± 5.49%). At weeks 8 and 12, the amount of new bone formation in the scaffold + MSCs group was significantly lower than in the scaffold-only group (week 8: 7.32% ± 4.93% versus 42.3% ± 4.427%, respectively; week 12: 17.24% ± 6.88% versus 61.01% ± 5.28%, respectively). Similar results were found for the percentage of bone mineralization, with significantly higher values in the scaffold-only group than in the scaffold + MSCs group (week 8: 40.51% ± 5.36% versus 7.71% ± 3.79%, respectively; week 12: 63.14% ± 5.49% versus 15.21% ± 6.49%, respectively).

Histologic Analysis

To investigate the remodeled tissue within the bone defect, slides were stained with H&E reagent. In the control group (Fig. 5A, B), we observed the presence of nonmineralized healing connective tissue and a few blood vessels (Fig. 5B, black arrow) in the area of the defect, together with mature bone regeneration at the defect's margin. In the scaffold-only group, H&E staining revealed that the defect was full of fibrous tissue (Fig. 5C, D). Finally, H&E staining of the samples from the scaffold + MSCs group revealed new bone formation in the center of the defect (areas stained in pink–red and marked with an asterisk in Fig. 5E, F). Bone appeared to have been regenerated in the middle of the implant. These histologic results confirmed the µCT data on the newly mineralized bone and provided additional information on the nature of the

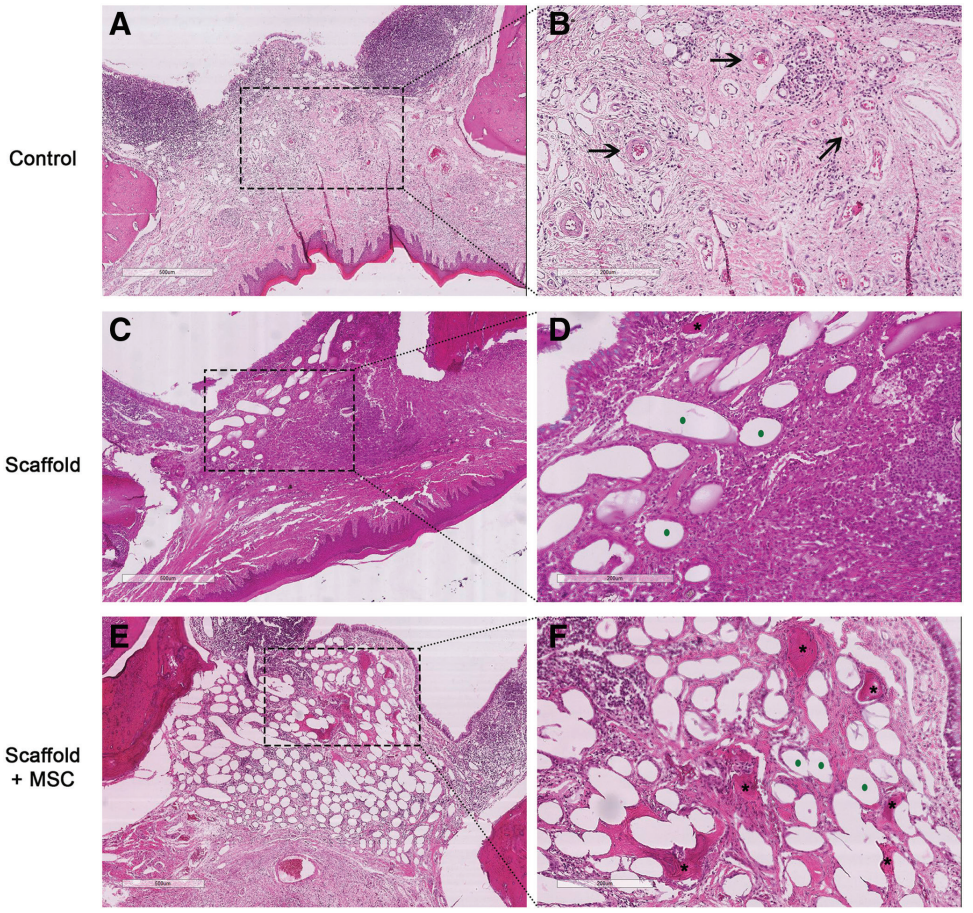

Fig. 5. Representative coronal histologic sections of the repaired defect in each group, 12 weeks after surgery (H&E staining). A and B, No graft (controls). C and D, Grafted with scaffold only. E and F, Grafted with MSC-seeded scaffold. The right-hand panels (D–F) correspond to higher magnifications (scale bar = 200 µm) of the areas shown in the left panels (A–C: scale bar = 500 µm). Black arrows indicate blood vessels, black stars indicate newly formed bone, and green dots indicate the scaffold's alginate fibers.

nonmineralized tissue. Alginate fibers were always present in the filled defect (Fig. 5D, F, green points).

DISCUSSION

Appropriate animal models are essential for testing new materials for tissue engineering and bone grafting therapy; the goal is to mimic the symptoms and/or anatomic consequences observed in patients. In the present study, we developed a highly reproducible rat model of a critical-sized cleft palate defect. Due to the difficulty of the surgical procedure, few small animal models of cleft palate have been developed. Teratogenic[22] and transgenic mouse cleft models[23,24] have been established but have not been used in the development of new bone graft therapies, probably because of the small size of the maxilla in the mouse and variability in the cleft's size and anatomic site. Hence, surgical cleft models were considered to be more suitable for testing the efficacy of new biomaterials for bone grafting,[25,26] as long as the surgically created defects have a critical size and do not heal spontaneously in the absence of treatment.[27]

However, it is well known that the presentation of cleft palate in humans is more variable than in the mouse or the rat. We presumed that our animal model, like other animal models of cleft palate, simulated certain characteristics of the human congenital cleft palate but not others. Furthermore, our experimental protocol may have influenced the results. In the present study, we assumed that the defect would heal within 12 weeks of treatment—the usual end point in this type of study.[17,28,29] However, it might be that in vivo, grafted cell-seeded scaffolds require more time for bone regeneration and thus a positive effect. To test this hypothesis, we will have to monitor animals with bioengineered tissue grafted for at least 6 months (as already suggested by Martin-Piedra et al[17]). Furthermore, self-healing capacity might also vary according to the lesion's site in the oral cavity,[25] and the high chewing pressure exerted on the wound area might partly account for our observations. Although the provision of soft food might overcome this limitation,[27,30] the animals in our experiment refused this type of chow. For patients, the wound can be covered and thus protected after the grafting.[31] Accordingly, we consider that this side effect could be avoided in clinical practice.

There is still no consensus today on which scaffold materials are most suitable for bone regeneration in the oral cavity. In clinical practice, hydrogels are widely used as bone substitutes and, in some cases, have been applied in cleft palate repair.[17,18] In previous work, we developed a new alginate-based hydrogel with high angiogenic and osteogenic potential (submitted results). In the present work, in vivo implantation of this hydrogel, seeded or not with rat BM-MSCs, in the rat palate defect model resulted in complete healing of the palatal mucosa, with no retraction or complications such as nasal obstruction, bleeding, and infection.

Complete bone reunion of the artificial defect was not observed in any of the 3 treatment groups. From the eighth week onward, the percentage of bone filling in the scaffold-only group was greater than in the control (no scaffold) group. However, the absence of statistically significant differences between these 2 treatment groups might be due to the small sample size and the interindividual differences in reconstruction. In all 3 treatment groups, bone deposition started at the edge of the defect and progressed toward the center—as already reported for this type of therapeutic approach,[28,30] and demonstrating the hydrogel's good osteointegration properties.

Several preclinical transplantation studies have shown that scaffolds seeded with MSCs are better than acellular scaffolds for osteogenesis and bone formation.[32] The addition of cells in our model was associated with bone formation not only at the defect margins but also in the center of the defect; as already observed by Kittaka et al[33] with a different cell-seeded scaffold in a rat calvarial defect model. The presence of calcified material was observed only in the scaffold + MSCs group. MSCs have a predominant paracrine role in promoting the migration of endogenous cells to injured tissue[34] but may also contribute directly to bone repair.[35] In our experiment, we could not determine the origin of the cells constituting these new bone structures because we isolated BM-MSCs from syngeneic rats of the same sex. Hence, we cannot say whether or not the bone formation in our model was due to paracrine effects, trophic effects, and/or direct engraftment of transplanted cells.

The literature data on the effect of cell seeding in bone substitute are inconsistent. In a rat mandibular symphysis model, Yagyuu et al[35] found that adding bone marrow stromal cells to a β-tricalcium phosphate ceramic had a positive effect on bone healing. In rat palatal bone defects, significant hard palate regeneration was observed when animals received the scaffold (poly-L-lactic acid) plus osteogenically differentiated fat-derived stem cells.[29] However, the study by Conejero et al[29] was based on histologic studies only, and lacked a quantitative analysis. Conversely, a bovine hydroxyl apatite/collagen substitute, seeded with either undifferentiated or osteogenically differentiated MSCs, did not enhance osteogenesis in a rodent alveolar cleft model.[28] The disparities observed in vivo might be due to interstudy differences in the nature of the biomaterial, the cell type, the experimental model, and the length of follow-up. Hence, a direct comparison with the present study is difficult.

Taken as a whole, our results suggest that a novel alginate-based hydrogel is biocompatible and is able to integrate into host tissues. We demonstrated the hydrogel's advantages for tissue healing in a rat model with a surgically created cleft palate and its ability to form bone (especially in the center of the defect) when seeded with MSCs.

CONCLUSIONS

Taken as a whole, our results indicate that a bioengineered alginate-based hydrogel bone substitute can induce the generation of bone tissue. It can be easily adapted to the anatomic defect site and may constitute a new tool for cleft surgery. Before this technology can be transferred into a clinical setting, further studies, with a

longer follow-up period, and a larger sample size, will be carried out to optimize the complete closure of the defect and to elucidate the origin of the bone developed within the scaffold.

Sophie Le Ricousse, PhD
Direction de la Recherche et de l'Innovation
52 avenue André Morizet
92513 Boulogne-Billancourt CEDEX
France
E-mail: sophie.le.ricousse@u-picardie.fr

ACKNOWLEDGMENTS

We thank Les Laboratoires Brothier for funding, Julie Le Ber (Head of the PlatAnN: animal housing facility) for assistance with animal experiments, and Paulo Marcelo (Head of ICAP: Ingénierie Cellulaire et Analyses des Protéines facility).

REFERENCES

1. Dixon MJ, Marazita ML, Beaty TH, et al. Cleft lip and palate: understanding genetic and environmental influences. *Nat Rev Genet.* 2011;12:167–178.
2. Lee YH, Liao YF. Hard palate-repair technique and facial growth in patients with cleft lip and palate: a systematic review. *Br J Oral Maxillofac Surg.* 2013;51:851–857.
3. Scheuermann M, Vanreusel I, Van de Casteele E, et al. Spontaneous bone regeneration after closure of the hard palate cleft: a literature review. *J Oral Maxillo Surg.* 2019;77:1074.e1–1074.e7.
4. Gładysz D, Hozyasz KK. Stem cell regenerative therapy in alveolar cleft reconstruction. *Arch Oral Biol.* 2015;60:1517–1532.
5. Pilipchuk SP, Plonka AB, Monje A, et al. Tissue engineering for bone regeneration and osseointegration in the oral cavity. *Dent Mater.* 2015;31:317–338.
6. Padial-Molina M, O'Valle F, Lanis A, et al. Clinical application of mesenchymal stem cells and novel supportive therapies for oral bone regeneration. *Biomed Res Int.* 2015;2015:341327.
7. Kaigler D, Pagni G, Park CH, et al. Stem cell therapy for craniofacial bone regeneration: a randomized, controlled feasibility trial. *Cell Transplant.* 2013;22:767–777.
8. Behnia H, Khojasteh A, Soleimani M, et al. Repair of alveolar cleft defect with mesenchymal stem cells and platelet derived growth factors: a preliminary report. *J Craniomaxillofac Surg.* 2012;40:2–7.
9. Bajestan MN, Rajan A, Edwards SP, et al. Stem cell therapy for reconstruction of alveolar cleft and trauma defects in adults: a randomized controlled, clinical trial. *Clin Implant Dent Relat Res.* 2017;19:793–801.
10. Kamal M, Ziyab AH, Bartella A, et al. Volumetric comparison of autogenous bone and tissue-engineered bone replacement materials in alveolar cleft repair: a systematic review and meta-analysis. *Br J Oral Maxillofac Surg.* 2018;56:453–462.
11. Wu C, Pan W, Feng C, et al. Grafting materials for alveolar cleft reconstruction: a systematic review and best-evidence synthesis. *Int J Oral Maxillofac Surg.* 2018;47:345–356.
12. Silva Gomes Ferreira PH, De Oliveira D, Duailibe De Deus CB, et al. Evaluation of the different biomaterials used in alveolar cleft defects in children. *Ann Maxillofac Surg.* 2018;8:315–319.
13. Pradel W, Lauer G. Tissue-engineered bone grafts for osteoplasty in patients with cleft alveolus. *Ann Anat.* 2012;194:545–548.
14. Pradel W, Tausche E, Gollogly J, et al. Spontaneous tooth eruption after alveolar cleft osteoplasty using tissue-engineered bone: a case report. *Oral Surg Oral Med Oral Pathol Oral Radiol Endod.* 2008;105:440–444.
15. Behnia H, Khojasteh A, Soleimani M, et al. Secondary repair of alveolar clefts using human mesenchymal stem cells. *Oral Surg Oral Med Oral Pathol Oral Radiol Endol.* 2009;108:e1–e6.
16. Hibi H, Yamada Y, Ueda M, et al. Alveolar cleft osteoplasty using tissue-engineered osteogenic material. *Int J Oral Maxillofac Surg.* 2006;35:551–555.
17. Martin-Piedra MA, Alaminos M, Fernandez-Valadès-Gamez R, et al. Development of a multilayered palate substitute in rabbits: a histochemical ex vivo and in vivo analysis. *Histochem Cell Biol.* 2017;147:377–388.
18. Liceras-Liceras E, Garzon I, Espana-Lopez A, et al. Generation of a bioengineered autologous bone substitute for palate repair: an in vivo study in laboratory animals. *J Tissue Eng Regen Med.* 2017;11:1907–1914.
19. Xie H, Wang Z, Zhang L, et al. Development of an angiogenesis-promoting microvesicle-alginate-polycaprolactone composite graft for bone tissue engineering application. *PeerJ.* 2016;4:e2040.
20. Neovius E, Lemberger M, Docherty Skogh AC, et al. Alveolar bone healing accompanied by severe swelling in cleft children treated with bone morphogenetic protein-2 delivered by hydrogel. *J Plast Reconstr Aesthet Surg.* 2013;66:37–42.
21. Lack S, Girardière C, Devauchelle B, et al. "Matrice pour la préparation d'une composition de regeneration cellulaire, tissulaire et/ou osseuse." FR Patent 1854630. Issued May 30, 2018.
22. Yamada T, Mishima K, Fujiwara K, et al. Cleft lip and palate in mice treated with 2,3,7,8-tetrachlorodibenzo-p-dioxin: a morphological in vivo study. *Congenit Anom (Kyoto).* 2006;46:21–25.
23. Gong SG, White NJ, Sakasegawa AY. The Twirler mouse, a model for the study of cleft lip and palate. *Arch Oral Biol.* 2000;45:87–94.
24. Juriloff DM, Harris MJ. Mouse genetic models of cleft lip with or without cleft palate. *Birth Defects Res A Clin Mol Teratol.* 2008;82:63–77.
25. Sun XC, Zhang ZB, Wang H, et al. Comparison of three surgical models of bone tissue defects in cleft palate in rabbits. *Int J Pediatr Otorhinolaryngol.* 2019;124:164–172.
26. Hong C, Quach A, Lin L, et al. Local vs. systemic administration of bisphosphonates in rat cleft bone graft: a comparative study. *PLoS One.* 2018;13:e0190901.
27. Mostafa NZ, Doschak MR, Major PW, et al. Reliable critical sized defect rodent model for cleft palate research. *J Craniomaxillofac Surg.* 2014;42:1840–1846.
28. Korn P, Hauptstock M, Range U, et al. Application of tissue engineered bone grafts for alveolar cleft osteoplasty in a rodent model. *Clin Oral Invest.* 2017;21:2521–2534.
29. Conejero JA, Lee JA, Parrett BM, et al. Repair of palatal bone defects using osteogenically differentiated fat-derived stem cells. *Plast Reconstr Surg.* 2006;117:857–863.
30. Mostafa NZ, Talwar R, Shahin M, et al. Cleft palate reconstruction using collagen and nanofiber scaffold incorporating bone morphogenetic protein in rats. *Tissue Eng Part A.* 2015;21:85–95.
31. Neiva C, Dakpe S, Gbaguadi C, et al. Calvarial periosteal graft for second-stage palate surgery: a preliminary report. *J Craniomaxillofac Surg.* 2014;42:e117–e124.
32. Mauney JR, Volloch V, Kaplan DL. Role of adult mesenchymal stem cells in bone tissue engineering applications: current status and future prospects. *Tissue Eng.* 2005;11:787–802.
33. Kittaka M, Kajiya M, Shiba H, et al. Clumps of a mesenchymal stromal cell/extracellular matrix complex can be a novel tissue engineering therapy for bone regeneration. *Cytotherapy.* 2015;17:860–873.
34. Gnecchi M, Danieli P, Malpasso G, et al. Paracrine mechanisms of mesenchymal stem cells in tissue repair. *Methods Mol Biol.* 2016;1446:123–146.
35. Yagyuu T, Kirita T, Hattori K, et al. Unique and reliable rat model for the assessment of cell therapy: bone union in the rat mandibular symphysis using bone marrow stromal cells. *J Tissue Eng Regen Med.* 2015;9:276–285.